Coupled Finite Element - Scaled Boundary Finite Element Method for Transient Analysis of Dam-Reservoir Interaction

Shangming Li

Institute of Structural Mechanics, China Academy of Engineering Physics,
Mianyang City, Sichuan Province, 621900, China
hustmingsl@126.com

Abstract. The scaled boundary finite element method (SBFEM) was extended to solve dam-reservoir interaction problems in the time domain, where dams were flexible and the fluid in reservoir was semi-infinite and compressible. Transient responses of dam-reservoir systems subjected to horizontal ground motions were analyzed based on the SBFEM and finite element method (FEM) coupling method. A dam was modeled by FEM, while the whole fluid in reservoir was modeled by the SBFEM alone or a combination of FEM and SBFEM. Two benchmark examples were considered to check the accuracy of the SBFEM-FEM coupling method. For a vertical dam-reservoir system, the semi-infinite fluid with a uniform cross section was modeled by the SBFEM alone. For non-vertical dam-reservoir systems, the fluid was divided into a near-field FEM domain and a far-field SBFEM domain. The geometry of near field is arbitrary, and the far field is a semi-infinite prism. Their numerical results obtained through the presented method were compared with those from analytical or substructure methods and good agreements were found.

Keywords: SBFEM; SBFEM-FEM coupling; dam-reservoir system; ground motions; transient analysis.

1 Introduction

A dam-reservoir system subjected to ground motions is often a major concern in the design. To ensure that dams are adequately designed for, the hydrodynamic pressure distribution along the dam-reservoir interface must be determined for assessment of safety. The assessment of safety of dam should include frequency and time domain analyses of dam-reservoir system.

In time-domain analyses, since an analytical solution is not available for dam-reservoir system with general or arbitrary geometry, numerical methods are often adopted. In numerical methods, a semi-infinite reservoir is usually divided into two parts: a near-field and a far-field domain. The near-field domain can be efficiently modeled by finite element method (FEM), while the effect of far-field domain can be represented by some kinds of transmitting boundary conditions (TBC) at the near-far-field interface. The most commonly-used TBC is Sommerfeld radiation condition [1],

B. Murgante et al. (Eds.): ICCSA 2011, Part IV, LNCS 6785, pp. 26–34, 2011.

which is very simply, but precautions have to be taken as the approach may introduce significant errors when the near-field domain is small. Sharan's TBC was developed [2]. Although it produced better results than Sommerfeld's, it does not represent the behaviour of the far-field domain well when the near-to-far-field interface is too near to the dam-reservoir interface. An efficient semi-analytical TBC [3] and later, its application [4] exhibited good results, but it required the full eigen-modes of the near-to-far-field interface. Other types of TBC were also developed [5-7]. Except for the TBC, boundary element method (BEM) was often adopted to model a semi-infinite reservoir [8-10]. BEM can generally yield more accurate results than TBC, but it requires a fundamental solution, which affects its applications.

In this study, the scaled boundary finite element method (SBFEM) was chosen to model the far-field domain. The SBFEM, which not only combines the advantages of FEM and BEM, but also avoids the disadvantages of BEM, was developed in [11] for an infinite soil-structure interaction. The efficiency for applications involving an infinite medium was also validated in [11]. The SBFEM was extended to solve certain infinite fluid-structure interaction problems in [12], where the fluid medium was not layered. For layered fluid medium, some works about frequency analysis based on the SBFEM [13,14] for dam-reservoir systems were done. A hydrodynamic pressure on rigid dams was analyzed based on SBFEM for layered incompressible fluid medium. In the time domain, the SBFEM includes convolution integrals, which greatly affects its analysis efficiency. To improve the SBFEM analysis efficiency, a continued-fraction formulation [16] of SBFEM for time-domain analysis was proposed to avoid evaluating convolution integrals, and a diagonalization procedure [17] was proposed, whose calculation efficiency was found to be high, although it still included convolution integrals. With the improvement of SBFEM evaluation efficiency in the time domain, the SBFEM for time analysis will show gradually its advantages. An alternative method [18] for obtaining the responses in the time domain is to obtain the frequency response first and then transform it into the time response through the inverse Fourier transform. As the inverse Fourier transform was used and the eigenvalue problem of a coefficient matrix must be solved to obtain the frequency response for each excitation frequency, the accuracy and efficiency of the alternative method need further improved. Therefore, based on the diagonaliztion procedure [17], this paper presented a SBFEM-FEM coupling method to solve transient analysis of deformable dam-reservoir systems. Numerical results showed its accuracy.

2 Problem Statement

A dam-reservoir system shown in Fig.1 was considered, where a dam is deformable and the fluid in reservoir is inviscid isentropic with fluid particles undergoing only small displacements. Analytical solutions of dams with arbitrary geometry in the time domain have not been reported in literatures. To circumvent the difficulty, the fluid in reservoir is divided into two parts: a near-field and a far-field domain as shown in Fig.1. The interaction between the near-field domain and the far-field domain occurs at Interface 2, while the interaction between the dam and the fluid occurs at Interface 1. Of note, Interface 2 is chosen to be vertical and the reservoir bottom in the far-field domain is level and rigid. These assumptions are necessary in SBFEM formulations, because the SBFEM requires no energy to be radiated from the infinity towards the dam.

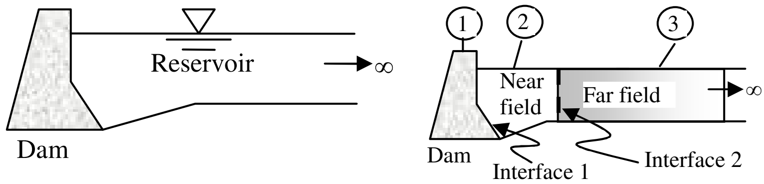

Fig. 1. Dam-reservoir system

3 Motion Equation of Dam

The motion equation for a dam subjected to both ground motions and external forces can be written in the standard finite element form as follows.

$$\mathbf{M}^d\ddot{\mathbf{U}}+\mathbf{C}^d\dot{\mathbf{U}}+\mathbf{K}^d\mathbf{U}=-\mathbf{M}^d\mathbf{R}\ddot{\mathbf{U}}_g+\mathbf{F}_e+\mathbf{F}_f \tag{1}$$

where $\mathbf{M}^d$, $\mathbf{C}^d$ and $\mathbf{K}^d$ denote the global mass, damping and stiffness matrices for the solid dam, respectively; $\ddot{\mathbf{U}}$, $\dot{\mathbf{U}}$ and $\mathbf{U}$ are the vectors of the nodal acceleration, velocity and displacement of dams, respectively; $\ddot{\mathbf{U}}_g$, $\mathbf{F}_e$ and $\mathbf{F}_f$ are the ground acceleration vector, the external force vector and the hydrodynamic force vector, respectively; and $\mathbf{R}$ denotes the acceleration transformation matrix. In Eq.(1), all matrices and vectors except $\mathbf{U}$ and $\mathbf{F}_f$ can be derived in the standard manner using the traditional finite element procedures. It leads to an expression such that the displacement $\mathbf{U}$ is a function of the hydrodynamic force $\mathbf{F}_f$.

4 FE Equation of Near Field

For a dam-reservoir system, the force term $\mathbf{F}_f$ on the right hand side of Eq.(1) is the force derived from the reservoir. It can be expressed as

$$\mathbf{F}_f=\sum_e\int_{\Gamma_1^e}\mathbf{N}^T\mathbf{N}_f\mathbf{p}_1 d\Gamma_1^e \tag{2}$$

where $\mathbf{N}$ and $\mathbf{N}_f$ denote the shape functions of a typical solid element for a dam and of a typical element for the near-field fluid medium, respectively; Γ_1 denotes Interface 1; the pressure $\mathbf{p}_1$ is a nodal pressure column vector, which is obtained from the near-field fluid domain. Note that $\mathbf{N}$ is not the same as $\mathbf{N}_f$.

After partitioning it into sub-matrices corresponding to variables at Interface 1, Interface 2 and other interior locations, the FE equation of Near field is written as

$$\begin{bmatrix} \mathbf{m}_{11}^f & \mathbf{m}_{12}^f & \mathbf{m}_{13}^f \\ \mathbf{m}_{21}^f & \mathbf{m}_{22}^f & \mathbf{m}_{23}^f \\ \mathbf{m}_{31}^f & \mathbf{m}_{32}^f & \mathbf{m}_{33}^f \end{bmatrix} \begin{Bmatrix} \ddot{\mathbf{\Phi}}_1 \\ \ddot{\mathbf{\Phi}}_2 \\ \ddot{\mathbf{\Phi}}_3 \end{Bmatrix} + \begin{bmatrix} \mathbf{k}_{11}^f & \mathbf{k}_{12}^f & \mathbf{k}_{13}^f \\ \mathbf{k}_{21}^f & \mathbf{k}_{22}^f & \mathbf{k}_{23}^f \\ \mathbf{k}_{31}^f & \mathbf{k}_{32}^f & \mathbf{k}_{33}^f \end{bmatrix} \begin{Bmatrix} \mathbf{\Phi}_1 \\ \mathbf{\Phi}_2 \\ \mathbf{\Phi}_3 \end{Bmatrix} = \begin{Bmatrix} \mathbf{V}_{n1} \\ \mathbf{V}'_{n2} \\ \mathbf{V}_{n3} \end{Bmatrix} \tag{3}$$

where the subscripts 1 and 2 refer to nodal variables at Interfaces 1 and 2, respectively; while the subscript 3 refers to other interior nodal variables in the near-field fluid domain. $\mathbf{m}$, $\mathbf{k}$ are the mass and stiffness matrices of Near field. $\mathbf{\Phi}$, $\mathbf{V}_n$ are the velocity potential and efficient nodal velocity. They can be obtained by traditional finite element procedures. At Interface 2, the near-field FEM-domain couples with the far-field SBFEM-domain.

5 SBFEM-FEM Coupling Formulation for Near Field

For Far field shown in Fig.1, its SBFEM discretization mesh is plotted in Fig.2. Each element at Interface 2 represents a sub-domain (i.e. sub-semi-infinite layered medium), so that the whole far-field domain is represented by an assemblage of elements at Interface 2 and its dynamic characteristics is described by the following SBFEM formulation

$$\mathbf{V}_{n2}(t) = \int_0^t \mathbf{M}^\infty(t-\tau)\ddot{\mathbf{\Phi}}_2(\tau)d\tau \tag{4}$$

$\mathbf{M}^\infty(t)$ is the dynamic mass matrix of the whole far-field domain. Upon discretization of Eq.(4) with respect to time and assuming all initial conditions equal to zero, one can get the following equation.

$$\mathbf{V}_{n2}^n = \mathbf{M}_1^\infty \dot{\mathbf{\Phi}}_2^n + \sum_{j=1}^{n-1}\left(\mathbf{M}_{n-j+1}^\infty - \mathbf{M}_{n-j}^\infty\right)\dot{\mathbf{\Phi}}_2^j \tag{5}$$

$\mathbf{M}_{n-j+1}^\infty = \mathbf{M}^\infty((n-j+1)\Delta t)$, $\mathbf{\Phi}_2^j = \mathbf{\Phi}_2(j\Delta t)$ and $\mathbf{V}_{n2}^n = \mathbf{V}_{n2}(n\Delta t)$ where Δt denotes an increment in time step. Details about $\mathbf{M}^\infty(t)$ can be found in [11, 17].

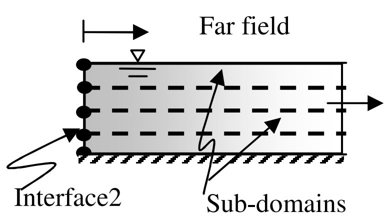

Fig. 2. SBFEM mesh of far field

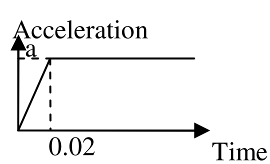

Fig. 3. Horizontal ramped acceleration

According to the kinematic continuity at Interface 2, one has

$$-\mathbf{V}_{n2}'^{n} = \mathbf{V}_{n2}^{n} = \mathbf{M}_1^{\infty}\dot{\mathbf{\Phi}}_2^{n} + \sum_{j=1}^{n-1}\left(\mathbf{M}_{n-j+1}^{\infty} - \mathbf{M}_{n-j}^{\infty}\right)\dot{\mathbf{\Phi}}_2^{j} \tag{6}$$

Substituting Eq.(6) into Eq.(3) and re-arranging leads to

$$\begin{bmatrix} \mathbf{m}_{11}^f & \mathbf{m}_{12}^f & \mathbf{m}_{13}^f \\ \mathbf{m}_{21}^f & \mathbf{m}_{22}^f & \mathbf{m}_{23}^f \\ \mathbf{m}_{31}^f & \mathbf{m}_{32}^f & \mathbf{m}_{33}^f \end{bmatrix} \begin{Bmatrix} \ddot{\mathbf{\Phi}}_1^n \\ \ddot{\mathbf{\Phi}}_2^n \\ \ddot{\mathbf{\Phi}}_3^n \end{Bmatrix} + \begin{bmatrix} \mathbf{0} & \mathbf{0} & \mathbf{0} \\ \mathbf{0} & \mathbf{M}_1^{\infty} & \mathbf{0} \\ \mathbf{0} & \mathbf{0} & \mathbf{0} \end{bmatrix} \begin{Bmatrix} \dot{\mathbf{\Phi}}_1^n \\ \dot{\mathbf{\Phi}}_2^n \\ \dot{\mathbf{\Phi}}_3^n \end{Bmatrix}$$
$$+ \begin{bmatrix} \mathbf{k}_{11}^f & \mathbf{k}_{12}^f & \mathbf{k}_{13}^f \\ \mathbf{k}_{21}^f & \mathbf{k}_{22}^f & \mathbf{k}_{23}^f \\ \mathbf{k}_{31}^f & \mathbf{k}_{32}^f & \mathbf{k}_{33}^f \end{bmatrix} \begin{Bmatrix} \mathbf{\Phi}_1^n \\ \mathbf{\Phi}_2^n \\ \mathbf{\Phi}_3^n \end{Bmatrix} = \begin{Bmatrix} \mathbf{V}_{n1}^n \\ -\sum_{j=1}^{n-1}\left(\mathbf{M}_{n-j+1}^{\infty} - \mathbf{M}_{n-j}^{\infty}\right)\dot{\mathbf{\Phi}}_2^{j} \\ \mathbf{V}_{n3}^n \end{Bmatrix} \tag{7}$$

where the superscript n denotes the instant at time $t = n\Delta t$. Note that a damping matrix appears on the left hand side of Eq.(7). It can be regarded as the damping effect derived from the far-field medium and imposed on the dam-reservoir system. Upon determining the velocity potential $\mathbf{\Phi}$ through Eq.(7), the fluid pressure $\mathbf{p}_1$ can be evaluated by

$$\mathbf{p}_1 = -\rho\dot{\mathbf{\Phi}}_1 \tag{8}$$

Note that $\mathbf{p}_1$ depends on the normal velocity v_{n1} at Interface 1, while the solution of Eq.(1) including v_{n1} also depends on $\mathbf{p}_1$. Therefore, Eq.(1) and Eq.(7) form a coupling system. Following the numerical procedure with a Newmark scheme, one can solve the coupling system by assuming

$$\mathbf{p}_1(t) = f\left(v_{n1}^{t}\right) \approx f\left(v_{n1}^{t-\Delta t}\right) \tag{9}$$

where f denotes a function. If the time increment Δt is small, accurate results can be obtained. However, if Δt is relatively large, an iteration scheme should be used in each time step, i.e., a term ${}^{t}v_{n1}^{j-1}$ is used instead of $v_{n1}^{t-\Delta t}$ in the global iteration scheme, where j denotes the jth iteration within a time step. Its corresponding formulation can be found in [12].

6 Numerical Examples

Consider transient responses of dam-reservoir systems where dams were subjected to horizontal ground acceleration excitations shown in Fig.3 and Fig.4. In the transient analysis, only the linear behavior was considered, the free surface wave effects and the reservoir bottom absorption were ignored, and the damping of dams was excluded. Newmark's time-integration scheme was used to solve FE equations (Eq.(1) and Eq.(7)). Newmark integration parameters $\alpha = 0.25$ and $\delta = 0.5$.

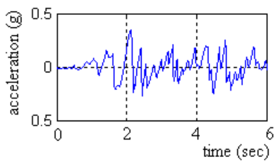

Fig. 4. El Centro N-S horizontal acceleration

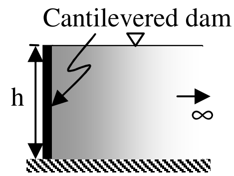

Fig. 5. Vertical dam-reservoir system

6.1 Vertical Dam

As the cross section of the vertical dam-system as shown in Fig.5 is uniform, a near-field fluid domain is not necessary and the whole reservoir can be modeled by a far-field domain alone. Its transient response was solved through coupling Eqs.(1) and (5). Sound speed in the reservoir is 1438.656*m/s* and the fluid density ρ is 1000kg/m^3. The weight per unit length of the cantilevered dam is 36000*kg/m*. The height of the cantilevered dam h is equal to 180*m*. The dam was modeled by 20 numbers of simple 2-noded beam elements with rigidity EI (=9.646826x10^{13} Nm^2), while the whole fluid domain was modeled by 10 numbers of SBFEM 3-noded elements, whose nodes matched side by side with nodes of the dam. In this problem, the shear deformation effects were not included in the 2-noded beam elements. Time step increment was 0.005*sec*. Results for the pressure at the heel of dam for ramped acceleration obtained by using a "no-iteration" scheme in Eq.(9) and an iteration scheme were plotted in Fig.6a. Results at late time from no-iteration scheme were divergent, whereas results obtained by both schemes were the same at early time. As such, an iteration scheme was adopted in the following studies. Pressures at the heel of dam obtained from the SBFEM coupling FEM procedure and an analytical method [3] were shown in Fig.6b. The SFEM-FEM solutions were very close to analytical solutions.

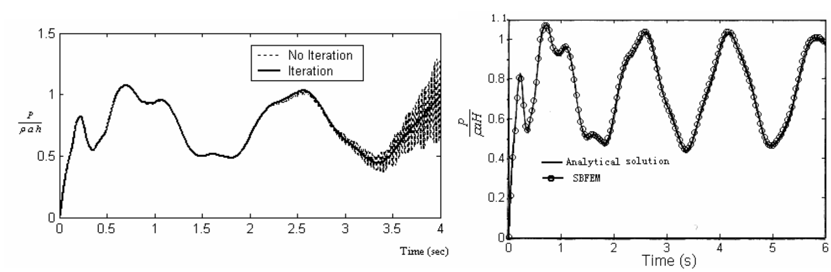

(a) (b)

Fig. 6. Pressures at the heel of dam subjected to horizontal ramped acceleration

6.2 Gravity Dam

This example was analyzed to verify the accuracy and efficiency of the SBFEM-FEM coupling formulation (Eq.(1) and Eq.(7)) for a dam-reservoir system having arbitrary slopes at the dam-reservoir interface. The density, Poisson's ratio and Young's modulus of the dam are 2400 kg/m^3, 0.2 and 3.43x10^{10} N/m^2, respectively. The fluid density ρ is 1000 kg/m3, and wave speed in the fluid is 1438.656m/s. The height of the dam H is 120m. A typical gravity-dam-reservoir system and its FEM and SBFEM meshes were shown in Fig.7.The dam and the near-field fluid were discretized by FEM, while the far-field fluid was discretized by the SBFEM. 40 numbers and 20 numbers of 8-noded elements were used to model the dam and the near-field fluid domain, respectively, while 10 numbers of 3-noded SBFEM elements were employed to model the whole far-field fluid domain. Note that the size of the near-field fluid domain can be very small, which was proven in the literature [14]. In this example, the distance between the heel of the dam and the near-far-field interface was 6m (=0.05H). The pressure at the heel of the gravity dam caused by the ground acceleration shown in Figs.3 and 4 were plotted in Fig.8. The time increment was 0.002sec. Results from SBFEM and FEM coupling procedure were very close to solutions from the sub-structures method [4].

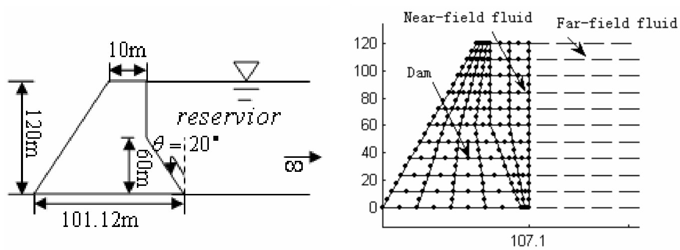

Fig. 7. Gravity dam-reservoir system and its FEM-SBFEM mesh

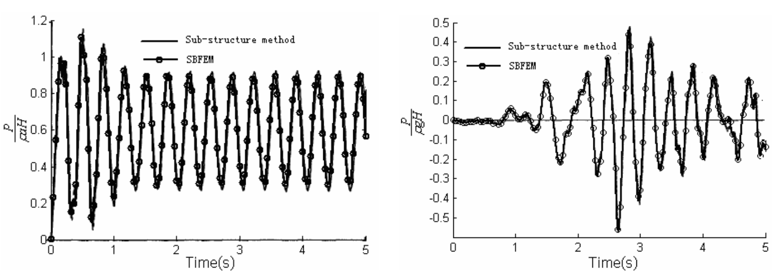

(a) Ramped acceleration (b) El Centro acceleration

Fig. 8. Pressure at the heel of gravity dam subjected to horizontal acceleration

The displacements at the top of vertical and gravity dams subjected to ramped acceleration were plotted in Fig.9. The displacement solutions of vertical dam from the presented method are the same with analytical solutions. Fig.10 showed the displacement at the top of gravity dam subjected to the El Centro N-S horizontal acceleration. The displacements obtained by the present method agreed well with sub-structure method's results [4], especially at early time.

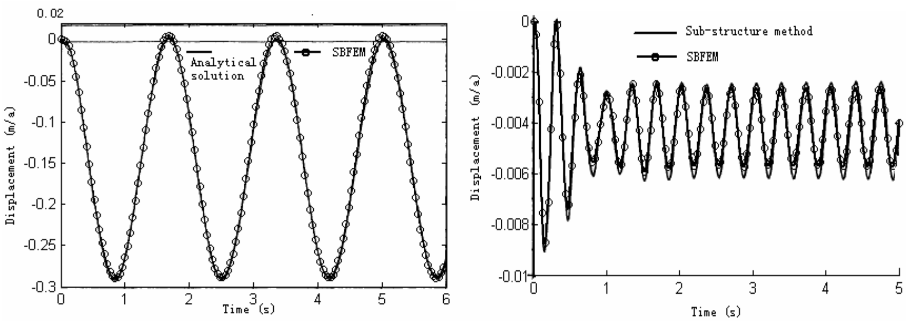

(a) Vertical dam (b) Gravity dam

Fig. 9. Displacement at top of dam subjected to horizontal ramped acceleration

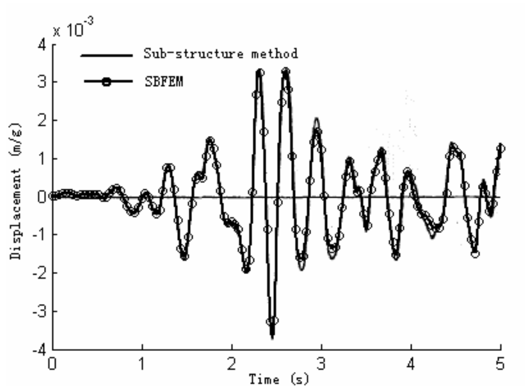

Fig. 10. Displacement at top of gravity dam subjected to horizontal El Centro acceleration

7 Conclusions

The SBFEM was employed in conjunction with FEM to solve the dam-reservoir interaction problems in the time domain. A coupled FE-SBFEM formulation was presented, which included a damping matrix induced by the damping effect of semi-infinite reservoir. The merits of the SBFEM in representing the unbounded fluid medium were illustrated through comparisons against benchmark solutions. Numerical results showed that its accuracy and efficiency of the coupled FE-SBFEM formulation for the transient analysis of dam-reservoir system. Of note, the SBFEM is a semi-analytical method. Its solution in the radial direction is analytical so that only a near field with a small volume is required. Compared to the sub-structure method [4], its formulations are in a simpler mathematical form and can be coupled with FEM easily and seamlessly.

Acknowledgments. This research is supported by the National Natural Science Foundation of China (No. 10902060) and China Postdoctoral Science Foundation (201003123), for which the author is grateful.

References

1. Sommerfeld, A.: Partial differential Equations in physics. Academic Press, New York (1949)
2. Sharan, S.K.: Finite element analysis of unbounded and incompressible fluid domains. International Journal for Numerical Methods in Engineering 21(9), 1659–1669 (1985)
3. Tsai, C.S., Lee, G.C., Ketter, R.L.: A semi-analytical method for time-domain analyses of dam-reservoir interactions. International Journal for Numerical Methods in Engineering 29, 913–933 (1990)
4. Tsai, C.S., Lee, G.C.: Time-domain analyses of dam-reservoir system. II: substructure method. Journal of Engineering Mechanics 117(9), 2007–2026 (1991)
5. Maity, S.K., Bhattacharyya, S.K.: Time-domain analysis of infinite reservoir by finite element method using a novel far-boundary condition. Finite Elements in Analysis and Design 32(2), 85–96 (1999)
6. Kucukarslan, S.: An exact truncation boundary condition for incompressible-unbounded infinite fluid domains. Applied Mathematics and Computation 163(1), 61–69 (2005)
7. Gogoi, I., Maity, D.: A non-reflecting boundary condition for the finite element modeling of infinite reservoir with layered sediment. Advances in Water Resources 29, 1515–1527 (2006)
8. Czygan, O., Von, E.O.: Fluid-structure interaction by coupling BEM and nonlinear FEM. Engineering Analysis with Boundary Elements 26, 773–779 (2002)
9. Dominguez, J., Maeso, O.: Earthquake analysis of arch dams. dam-water-foundation interaction. Journal of Engineering Mechanics-ASCE 119, 513–530 (1993)
10. Dominguez, J., Gallego, R., Japon, B.R.: Effects of porous sediments on seismic response of concrete gravity dams. Journal of Engineering Mechanics-ASCE 123, 302–311 (1997)
11. Wolf, J.P., Song, C.: Finite-Element Modeling of Unbounded Media. Wiley, Chichester (1996)
12. Fan, S.C., Li, S.M., Yu, G.Y.: Dynamic fluid-structure interaction analysis using boundary finite element method/finite element method. Journal of Applied Mechanics 72(4), 591–598 (2005)
13. Fan, S.C., Li, S.M.: Boundary finite-element method coupling finite-element method for steady-state analyses of dam-reservoir systems. Journal of Engineering Mechanics-ASCE 134, 133–142 (2008)
14. Li, S.M., Liang, H., Li, A.M.: A semi-analytical solution for characteristics of a dam-reservoir system with absorptive reservoir bottom. Journal of Hydrodynamics 20(6), 727–734 (2008)
15. Du, J.G., Lin, G., Hu, Z.Q.: Hydrodynamic pressure on dams based on SBFEM. Geotechnical Special Publication, Num. 151, 262–269 (2006)
16. Bazyar, M.H., Song, C.M.: A continued-fraction-based high-order transmitting boundary for wave propagation in unbounded domains of arbitrary geometry. International Journal for Numerical Methods in Engineering 74, 209–237 (2008)
17. Li, S.M.: Diagonalization procedure for scaled boundary finite element method in modelling semi-infinite reservoir with uniform cross section. International Journal for Numerical Methods in Engineering 80(5), 596–608 (2009)
18. Wang, Y., Lin, G., Hu, Z.Q.: A Coupled FE and Scaled Boundary FE-Approach for the Earthquake Response Analysis of Arch Dam-Reservoir-Foundation System. In: IOP Conference Series: Materials Science and Engineering, vol. 10, pp. 1–10 (2010)